MLSE AND MMSE SUBCHANNEL EQUALIZATION FOR FILTER BANK BASED MULTICARRIER SYSTEMS: CODED AND UNCODED RESULTS

Leonardo G. Baltar, Amine Mezghani, Josef A. Nossek

Institute for Circuit Theory and Signal Processing
Technische Universität München
Arcisstr. 21, 80290 München, Germany
Email: {leo.baltar, amine.mezghani, josef.a.nossek}@tum.de

ABSTRACT

Filter Bank Based Multicarrier (FBMC) systems appears to be the best choice to replace Cyclic Prefix (CP) based Orthogonal Frequency Division Multiplexing (OFDM) as the physical layer of future wireless communications devices.

Some equalizer solutions for FBMC systems already exist. Among them, the equalizers minimizing the mean square error (MMSE) criterion show the best trade-off between complexity and performance. In this work we evaluate the uncoded BER performance of FBMC systems with two kinds of receivers: the per-subchannel MMSE Linear Equalizer (LE) and a maximum likelihood sequence estimator (MLSE). Moreover, we compare the coded and uncoded BER of FBMC with CP-OFDM in a configuration where both systems have the same spectral efficiency. From our results we can conclude that the MMSE LE achieves a satisfactory performance compared to the MLSE but with a much lower computational complexity. We also show that the FBMC scheme reduces the energy per bit by 2.5 dB compared to CP-OFDM under the same spectral efficiency.

1. INTRODUCTION

The physical layer of future wireless communications systems is expected to provide an even higher data rate when compared with current schemes. Multicarrier (MC) based systems have shown to be the best choice for this requirement because of its many advantages. The basic principle of MC to divide the frequency spectrum into many narrow subchannels is not new, but only in the last decade a widespread use in practical systems could be observed. There are many classes of MC systems, but the CP-OFDM is certainly the most investigated one. It offers the advantage of efficient and simple implementation and the channel equalization becomes a trivial task. As a result of the insertion of redundancy (CP), only one tap per subchannel is necessary to compensate the frequency selectivity of the channel. The drawbacks of CP-OFDM compared to other modulation schemes include a loss in spectral efficiency, as a consequence of the CP insertion, a higher level of out-of-band radiation, since the subcarriers have a sinc-like frequency behavior, and a higher sensitivity to narrowband interferers when the synchronization is not perfect, because the low attenuation of the sidelobes implies in an frequency undesired overlap of the subchannels.

CP-OFDM is based on the general MC concept of modulated transmultiplexers (TMUX), which are composed of exponentially modulated analysis and synthesis filter banks, what we call FBMC systems. Maximally decimated filter banks are of particular interest. Instead of using a rectangular window for pulse shaping, a finite impulse response (FIR) prototype filter that has a longer impulse response than the symbol period, i. e. the number of filter coefficients is higher than the number of subchannels M, is modulated by complex exponentials to form each subchannel. Because of its longer length, the filters can be more concentrated in the frequency domain and the subchannels are shaped to overlap only with the contiguous ones. The prototype filter is also chosen to fulfill the Nyquist Intersymbol Interference (ISI) criterion, so that its impulse response has zero crossings at the symbol period T. But it is known from filter bank [1] and communication theory [2] that, in a complex modulated and critically sampled TMUX, if the input signals are complex and in order to achieve the perfect reconstruction or ISI- and ICI-free conditions, the real and imaginary parts of the input signals must be staggered by $T/2$, resulting in the so called Offset Quadrature Amplitude Modulation (OQAM).

The equalization problem in FBMC systems is still an active research topic. We focus here on solutions that depend only on the output signals of each subchannel. In this way per-subchannel equalizers work like single carrier (SC) equalizers for OQAM modulated symbols, but with the difference that Interchannel Interference (ICI) is present. Since noise cannot be considered white at the output of a filter with bandwidth smaller than the sampling frequency, this has to be considered in the equalizer design. Furthermore, in an FBMC system with OQAM input symbols the equalizer can be inserted in front of the de-staggering, leading to a fractionally spaced equalizer (FSE) working at a rate of $2/T$, where $1/T$ is the symbol rate.

In the classical literature of receivers for frequency selective channels, the MLSE equalizer is referred as the optimal receiver [3]. In addition to completely mitigating the ISI, those receivers make use of the time diversity inserted by the multipath channel. The main drawback and an obstacle to practical use of the MLSE is its computational complexity.

Some practical solutions for the problem of channel equalization already exist in the literature. In [4] the authors consider the equalizer optimization in the frequency domain, while in [5] a time domain optimization of the MMSE linear equalizer is presented. In [6] an MMSE decision feedback equalizer is derived.

In this paper we evaluate the uncoded bit error rate (BER) of FBMC systems by considering a comparison between the MLSE receiver adapted to the OQAM modulation and the unbiased MMSE linear equalizer. Moreover, we compare the coded and the uncoded BER of CP-OFDM and FBMC systems when both have the same data rate.

This work is organized as follows. In Section 2, we give an overview of the FB system model and an efficient struc-

ture for its realization. We describe in details, in Section 3, both the MLSE and the linear unbiased MMSE receivers. In Section 4, we show some simulation results and in Section 5 some conclusions are drawn.

2. OQAM FBMC SYSTEM MODEL AND STRUCTURE

A general overview of the FBMC system model is depicted in Fig. 1. The filter banks are employed in a transmultiplex architecture. At the transmitter a synthesis filter bank (SFB) performs a frequency division multiplexing (FDM) of the complex data symbols $d_k[m]$ into parallel subchannels of rate $1/T$. At the receiver, an analysis filter bank (AFB) separates the data from the single subchannels. In our model we include a frequency selective channel and an AWGN source between the SFB and the AFB.

We consider here an exponentially modulated filter bank both in SFB and AFB. This means that only one prototype low-pass filter has to be designed and the other subfilters are obtained by modulating it as follows

$$h_k[l] = h_0[l]\exp\left(\mathrm{j}\,2\pi kl/M\right), \quad l = -KM/2,\ldots,KM/2, \quad (1)$$

where $h_0[l]$ is the impulse response of the prototype filter, M is the total number of subcarriers and K is the time overlapping factor that determines how many blocks of symbols superpose each other. The prototype is a Nyquist-like filter usually with a roll-off factor $\rho = 1$. Consequently, only contiguous subchannels overlap in the frequency domain and the other subcarriers are attenuated by the good stopband behavior. Moreover, we will always consider here $K = 4$.

Since the prototype filter is longer then the number of subchannels M, and in order to maintain the orthogonality between all the subchannels and for all time instants, the input symbols $d_k[m]$ need to have its real and complex parts staggered by $T/2$ resulting in an OQAM modulation scheme [7]. The OQAM staggering for even indexed subchannels is depicted in Fig. 2. In odd indexed subchannels the delay of $T/2$ is located in the lower branch with purely imaginary symbols. At the receiver the OQAM demodulation is performed by transposing [8] the signal-flow in Fig. 2 and exchanging the blocks named Re and jIm.

The operation of upsampling and filtering each substream can be executed by employing an efficient structure of both SFB and AFB. This structure uses an inverse discrete Fourier transform (IDFT) to execute the modulation and a polyphase network at the transmitter as shown in Fig. 3, where $z_1 = \mathrm{e}^{\frac{sT}{2}}$, $z = \mathrm{e}^{\frac{sT}{M}}$, while s is the complex frequency variable, and $G_p^{(p1)}(z_1^2)$ are the p-th polyphase components of type 1 of the prototype $H_0(z_1)$ [8].

At the receiver a polyphase filtering is first executed then the DFT demodulates the single subchannels. The higher efficiency comes also from the deployment of a fast Fourier transform (FFT) to implement both IDFT and DFT.

It is possible to find in the literature even more efficient structures depending on the characteristics of the prototype filter, see [9].

3. PER-SUBCHANNEL EQUALIZATION

Because the frequency selective channel deforms the frequency response of the ideal subchannel, ISI and ICI will be encountered in each subchannel. In order to recover the

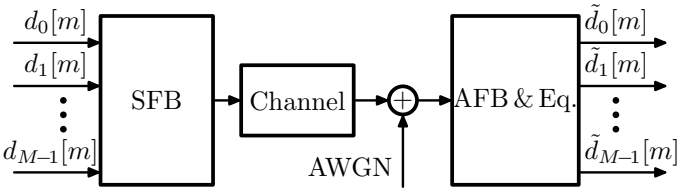

Figure 1: FBMC System Overview

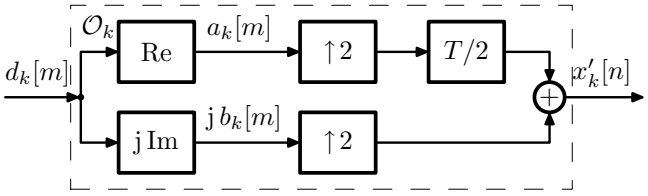

Figure 2: OQAM Staggering $\mathcal{O}_k$, k even

subchannel spectral shape, an equalizer has to be inserted at the receiver in front of the OQAM destaggering, i.e. its input and output samples have a period of $T/2$.

According to the selection of the prototype (see Sec. 2) it is reasonable to assume that on each subchannel only ICI from contiguous subchannels is present. This subchannel model is depicted in Fig. 4.

We collect the k-th subchannel output symbols from $y_k[n]$ to $y_k[n-N]$ in a vector $\boldsymbol{y}_k[n] \in \mathbb{C}^N$ and write it as a function of the three input signals and the noise. For this, we employ the convolution matrices $\boldsymbol{G}'_k$, $\boldsymbol{M}'_k$, $\boldsymbol{N}'_k \in \mathbb{C}^{N\times Q}$, $\boldsymbol{\Gamma}_k \in \mathbb{C}^{N\times M(K+N/2)+1}$, with $Q = N+L-1$, composed of the L long impulse responses $m'_k[n]$, $n'_k[n]$, $g'_k[n]$ from the input symbols and $\gamma'_k[l]$ from the noise as follows

$$\boldsymbol{y}_k[n] \approx \boldsymbol{G}'_k\boldsymbol{x}'_k[n] + \boldsymbol{M}'_k\boldsymbol{x}'_{k-1}[n] + \boldsymbol{N}'_k\boldsymbol{x}'_{k+1}[n] + \boldsymbol{\Gamma}_k\eta[l], \quad (2)$$

where $\eta[l] \in \mathbb{C}^{M(K+N/2)+1}$ and the vectors $\boldsymbol{x}'_{k-1}[n], \boldsymbol{x}'_k[n], \boldsymbol{x}'_{k+1}[n] \in \mathbb{C}^Q$ have components alternating between purely real or purely imaginary numbers as a result of the OQAM staggering. If the imaginary unit j is moved to the convolution matrices we can rewrite the received signal as

$$\boldsymbol{y}_k[n] \approx \boldsymbol{G}_k[n]\boldsymbol{x}_k[n] + \boldsymbol{M}_k[n]\boldsymbol{x}_{k-1}[n] + \boldsymbol{N}_k[n]\boldsymbol{x}_{k+1}[n] + \boldsymbol{\Gamma}_k\eta[l], \quad (3)$$

Note that now the vectors $\boldsymbol{x}_{k-1}[n], \boldsymbol{x}_k[n], \boldsymbol{x}_{k+1}[n] \in {}^{Q}$ contain only real numbers and the convolution matrices $\boldsymbol{G}'_k$[n], $\boldsymbol{M}'_k[n]$, $\boldsymbol{N}'_k[n] \in \mathbb{C}^{N\times Q}$ correspond to time-variant impulse responses.

Based on this subchannel model we consider two possible equalizer structures in the next subsections.

3.1 MLSE

First, let us consider the more sophisticated MLSE equalization for the FBMC system. The optimal MLSE receiver should take into account the output of all subchannels to find the most likely input symbols. The problem is that this joint ML decoding among all subcarriers is computationally infeasible. Nevertheless, since there is overlap only between

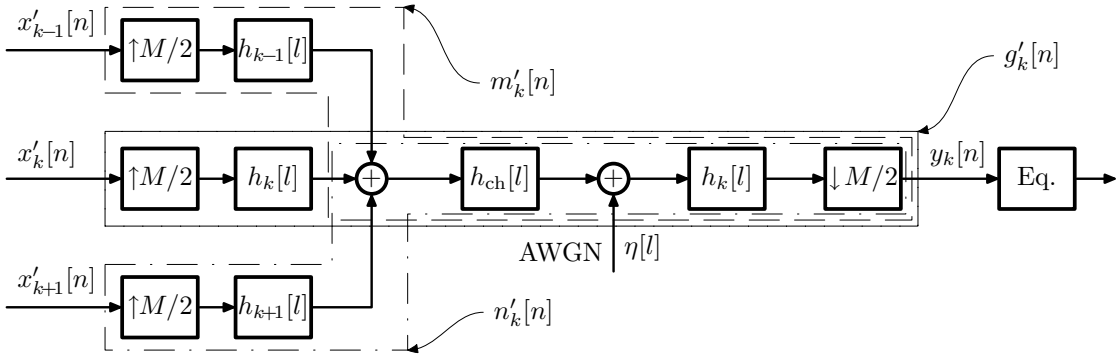

Figure 4: Subchannel Model for the FBMC System

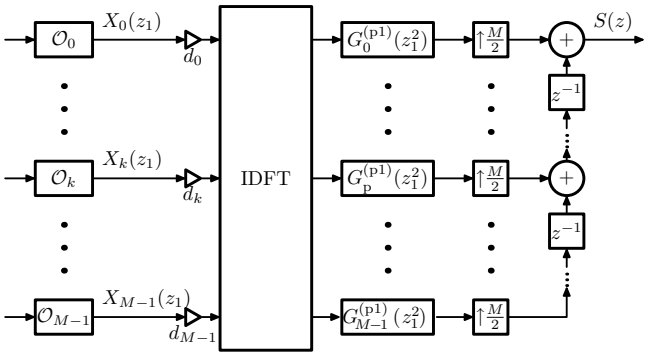

Figure 3: Efficient structure of the SFB

contiguous subchannels, the complexity can be reduced by using a two-dimensional Viterbi-like detector, but it still remains much more complex than a per-subchannel detector.

Therefore, for simplicity, the interference from the adjacent subcarriers is assumed to be Gaussian distributed, which means that we separately perform a suboptimal MLSE on each subcarrier. Furthermore, we ignore the fact the ICI is colored. In that case, the MLSE rule is only related to the impulse response $g'_k[n]$, whose length is denoted by L. For the case of OQPSK modulation, the trellis has 2^L states with only two possible transitions per state since the detection is carried out on a real representation of the data. The MLSE selects the input sequence $\hat{x}_k[0],...,\hat{x}_k[B]$ of length B that minimizes the cost

$$\mathscr{C}_k[B] = \sum_{m=0}^{B} \left| y_k[m] - \sum_{n=0}^{L-1} x_k[m-n] g_k\prime[n] \cdot \mathbb{I}(m-n) \right|^2, \quad (4)$$

where

$$\mathbb{I}(n) = \begin{cases} 1 & \text{for } n \text{ even}, \\ \mathrm{j} & \text{for } n \text{ odd}. \end{cases}$$

Hereby, the case distinction follows from the OQAM constellation structure and we assume the subcarrier index k to be odd. For even k, we just have to reverse the definition of $\mathbb{I}(n)$. More precisely, the MLSE rule (4) can be computed sequentially using the Viterbi algorithm as

$$\mathscr{C}_k[m] = \mathscr{C}_k[m-1] + \left| y_k[m] - \sum_{n=0}^{L-1} x_k[m-n] \bar{g}_k[m,n] \right|^2, \quad (5)$$

where $\bar{g}_k[m,n]$ represents a time-variant impulse response given by

$$\bar{g}_k[m,n] = \begin{cases} g'_k[n] & \text{for } m \text{ even}, \\ \mathrm{j} g'_k[n] & \text{for } m \text{ odd}, \end{cases}$$

and $x_k[n] \in \{\pm 1\}$ for the OQPSK case. In other words, the added single squared error term at time m to the cost at time $m-1$ has to be computed differently, depending on whether m is even or odd.

3.2 Unbiased MMSE Linear Equalization

In [5] we derived the MMSE linear equalizer $\boldsymbol{w}_k$ as

$$\boldsymbol{w}'_k = \left[\boldsymbol{H}_k \boldsymbol{H}_k^{\mathrm{T}} + \boldsymbol{F}_k \boldsymbol{F}_k^{\mathrm{T}} + \boldsymbol{R}_{\eta,k} \right]^{-1} \frac{\sigma_d}{\sqrt{2}} \boldsymbol{H}_k \boldsymbol{e}_\nu,$$

where $\boldsymbol{w}_k^{\prime,\mathrm{T}} = \begin{bmatrix} \boldsymbol{w}_k^{(R),\mathrm{T}} & \boldsymbol{w}_k^{(I),\mathrm{T}} \end{bmatrix}^{\mathrm{T}}$, $\boldsymbol{w}_k^{(R)} = \mathrm{Re}\{\boldsymbol{w}_k\}$, $\boldsymbol{w}_k^{(I)} = \mathrm{Im}\{\boldsymbol{w}_k\}$, and

$$\boldsymbol{H}_k = \frac{\sigma_d}{\sqrt{2}} \begin{bmatrix} \boldsymbol{G}_k^{(\mathrm{R})} \\ \boldsymbol{G}_k^{(\mathrm{I})} \end{bmatrix}, \qquad \boldsymbol{F}_k = \frac{\sigma_d}{\sqrt{2}} \begin{bmatrix} \boldsymbol{M}_k^{(\mathrm{R})} & \boldsymbol{N}_k^{(\mathrm{R})} \\ \boldsymbol{M}_k^{(\mathrm{I})} & \boldsymbol{N}_k^{(\mathrm{I})} \end{bmatrix},$$
$$\boldsymbol{R}_{\eta,k} = \frac{\sigma_\eta^2}{2} \boldsymbol{\Gamma}'_k \boldsymbol{\Gamma}_k^{\prime,\mathrm{T}}, \qquad \boldsymbol{\Gamma}'_k = \begin{bmatrix} \boldsymbol{\Gamma}_k^{(R)} & \boldsymbol{\Gamma}_k^{(I)} \\ \boldsymbol{\Gamma}_k^{(I)} & -\boldsymbol{\Gamma}_k^{(R)} \end{bmatrix},$$

while $\boldsymbol{G}_k^{(\mathrm{R})}$, $\boldsymbol{G}_k^{(\mathrm{I})}$ $\boldsymbol{M}_k^{(\mathrm{R})}$, $\boldsymbol{M}_k^{(\mathrm{I})}$, $\boldsymbol{N}_k^{(\mathrm{R})}$, $\boldsymbol{N}_k^{(\mathrm{I})}$, $\boldsymbol{\Gamma}_k^{(\mathrm{R})}$, $\boldsymbol{\Gamma}_k^{(\mathrm{I})}$ are the real and imaginary parts of the matrices $\boldsymbol{G}_k[n]$,$\boldsymbol{M}_k[n]$, $\boldsymbol{N}_k[n]$ and $\boldsymbol{\Gamma}_k[n]$. Moreover, $\sigma_d^2 = \mathrm{E}[d_k[m] d_k^*[m]]$ for the assumption of i.i.d. input symbols, $\sigma_\eta^2 = \mathrm{E}[\eta[m] \eta^*[m]]$ and $\boldsymbol{e}_\nu$ is the ν-th unit vector.

Given an equalizer impulse response for each subchannel, it can be shown that the MSE at its output is given by

$$\mathrm{MSE}_k = \sigma_d^2 (1 - \boldsymbol{w}'_k \boldsymbol{H}_k^{\mathrm{T}} \boldsymbol{e}_\nu). \quad (6)$$

On the other hand, the output of the MMSE equalizer is given by

$$z_k[m] = \alpha_k(d_k[m] + \mathrm{ISI}_k + \mathrm{ICI}_k + \eta_k[n]),$$

where ISI_k and ICI_k are the residual intersymbol and interchannel interference, respectively, while the factor $\alpha_k = \mathrm{E}[z_k|d_k]/d_k < 1$ is related to the bias inserted by this equalizer, as it is well-known that the linear MMSE equalizer is biased. Consequently, it can be demonstrated that the Signal to Interference plus Noise Ratio (SINR) at the output of the MMSE LE is [10]

$$\mathrm{SINR}_k = \frac{\sigma_d^2}{\mathrm{MSE}_k} - 1.$$

Moreover, as shown in [10], the bias is defined as

$$\alpha_k = \frac{1}{1 + (\mathrm{SINR}_k)^{-1}}.$$

A simple way to force the MMSE equalizer to become unbiased is by simply multiplying its output by α_k^{-1}. As a result, the bias removal coefficient is given by

$$\alpha_k^{-1} = \frac{\sigma_d^2}{\sigma_d^2 - \mathrm{MSE}_k}$$

It is worth noting that although the bias removal reduces the symbol estimation error, it increases the MSE in each subchannel. The new MSE becomes

$$\mathrm{MSE}_{k,U} = \frac{1}{\alpha_k}\mathrm{MSE}_k = \frac{\sigma_d^2 \mathrm{MSE}_k}{\sigma_d^2 - \mathrm{MSE}_k}$$

Furthermore, we would like to comment that in the case of CP-OFDM, the trivial one-tap MMSE unbiased equalizer is equal to the zero forcing equalizer. The latter is widely accepted as the standard one-tap equalizer for CP-OFDM.

4. SIMULATION RESULTS

In our simulations we have considered the FBMC system described in Section 2. The prototype was obtained by the frequency sampling method described in [11] and its magnitude frequency response is shown in Fig. 5. The channel between synthesis and analysis FBs is modeled as an FIR filter to reproduce the effects of multipath propagation encountered in wireless communication environments. For the matter of comparison, we have employed at the receiver both MLSE and Unbiased MMSE linear equalizer to compensate for the frequency selectivity of the channel.

In the first example we have employed the parameters in Table 1. Fig. 6 shows a comparison of the uncoded BER between the MMSE Linear Equalizer and two variants of the MLSE equalizer. The curve denoted MLSE ICI corresponds to the case where the ICI is not removed before the sequence estimation, but just seen as Gaussian noise. The curve denoted MLSE corresponds to the case where ICI is completely removed from the received signal unrealistically assuming that the receiver perfectly knows it. This is consequently a performance lower bound for a feasible MLSE.

The analytical probability of error is also depicted in Fig. 6. For this computation, we have assumed that the sum

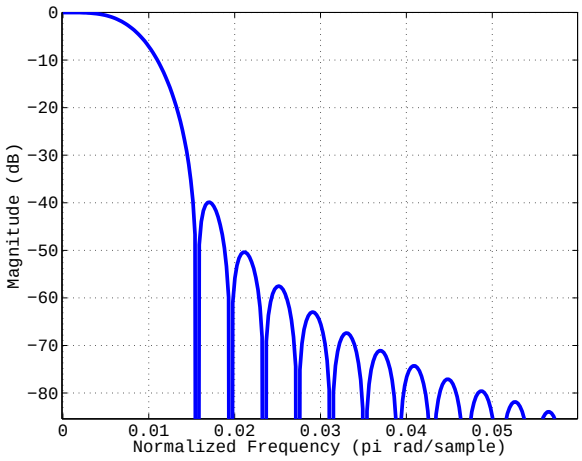

Figure 5: FIR prototype filter magnitude response for $M = 128$, $K = 4$, length $KM + 1$ and designed according to [11]

Parameter	Value
Modulation	QPSK
Total number of subchannels	$M = 128$
Data filled subchannels	$M_{\text{data}} = 96$
Subchannel spacing	$\Delta f = 87.2$ kHz
Total bandwidth	BW $= 10$ MHz
Sampling period	$T_s = 89.28$ ns
Equalizer length	$N = 21$
Channel model	ITU Vehicular B static
RMS delay spread	$\tau_{\text{RMS}} = 4\,\mu$s
Symbols per subchannel	100
Channel realizations	100

Table 1: Parameters for BER comparison of FBMC receivers

of the residual ISI, ICI and noise at the output of the equalizer are Gaussian distributed. Consequently the probability of error was calculated for an AWGN channel on each subchannel and for each channel realization. The variance of that interference-plus-noise source is given by the MSE in Eq. (6).

We can see that for low values of E_b/N_0 (Energy per bit over the one sided noise power spectral density) both MMSE and MLSE equalizers present similar results, only for higher values of E_b/N_0, the MLSE without ICI presents significant improvements. Clearly, this improved performance comes at the price of an impractical increase in the computational complexity.

As a second example, we have considered a comparison between the coded and uncoded BER for both FBMC employing 16-QAM and CP-OFDM employing 32-QAM. We have used a convolutional encoder and a soft decoder. All the other parameters are shown in Table 2 and the results are depicted in Fig. 7. By choosing different QAM alphabets both systems will possess the same spectral efficiency in bits/Hz. It should be clear that CP-OFDM loses in spectral efficiency proportionally to the length of the CP.

From the simulation in Fig. 7 it is possible to see that the FBMC system allows a reduction of 2.5 dB in the transmitted power to achieve the same data rate and BER performance of a similar CP-OFDM system.

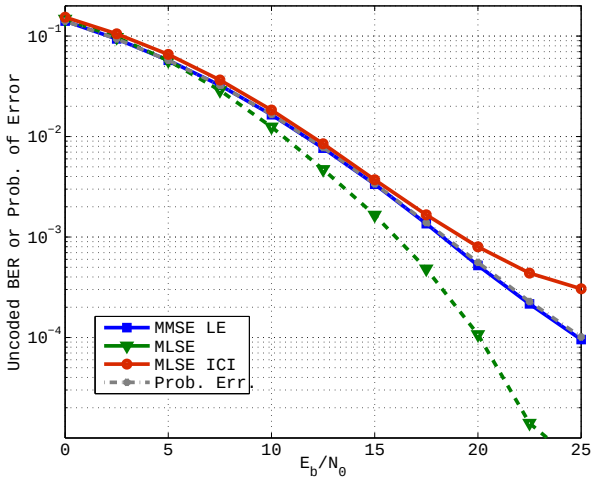

Figure 6: Uncoded BER comparison between MMSE Linear Equalizer and MLSE. Parameterization from Table 1.

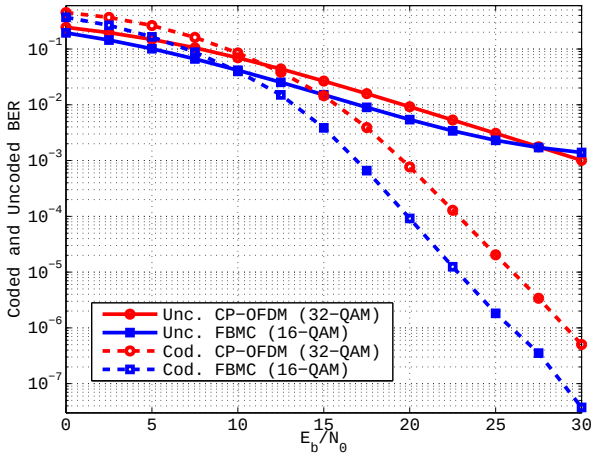

Figure 7: Uncoded and coded BER comparison between FBMC with LE and OFDM

Parameter	Value
Total number of subchannels	$M = 1024$
Data filled subchannels	$M_{\text{data}} = 768$
Subchannel spacing	$\Delta f = 10.9$ kHz
Total bandwidth	BW $= 10$ MHz
Sampling period	$T_s = 89.28$ ns
CP length	$T_{\text{CP}} = 22.85\,\mu$s $(1/4)$
Equalizer length	$N = 5$
Channel model	ITU Vehicular B static
RMS delay spread	$\tau_{\text{RMS}} = 4\,\mu$s
Symbols per subchannel	1000
Channel realizations	200
Code rate, R	$1/2$
Code polynomials	$1+D^1+D^2+D^3+D^6$
	$1+D^2+D^3+D^5+D^6$
Type of decoder	Max-log-MAP algorithm

Table 2: Parameters for BER comparison between FBMC and CP-OFDM

5. CONCLUSIONS

We presented in this work a comparison of the BER performance between the linear MMSE equalizer and the MLSE receiver for FBMC systems. The MMSE linear equalizer shows a performance very close to the MLSE for low values of E_b/N_0 but at a much lower computational complexity.

We also compared the uncoded and coded BER performance between FBMC and CP-OFDM in a wireless communications scenario. From the simulations results we can conclude that the FBMC system presents an advantage of 2.5 dB compared to a CP-OFDM system.

Acknowledgment

This work was partially supported by the European Commission under the Project PHYDYAS (FP7-ICT-2007-1-211887).

REFERENCES

[1] T. Karp and N. J. Fliege, "Modified DFT filter banks with perfect reconstruction," *IEEE Trans. Circuits Syst. II*, vol. 46, no. 11, pp. 1404 –1414, Nov 1999.

[2] P. Siohan, C. Siclet, and N. Lacaille, "Analysis and design of OFDM/OQAM systems based on filterbank theory," *IEEE Trans. Signal Processing*, vol. 50, no. 5, pp. 1170–1183, May 2002.

[3] J. G. Proakis, *Digital Communications*, 4th ed. New York, NY: McGraw-Hill, 2001.

[4] T. Ihalainen, T. H. Stitz, M. Rinne, and M. Renfors, "Channel equalization in filter bank based multicarrier modulation for wireless communications," *EURASIP J. Appl. Signal Process.*, vol. 2007, no. 1, pp. 140–140, 2007.

[5] D. S. Waldhauser, L. G. Baltar, and J. A. Nossek, "MMSE subcarrier equalization for filter bank based multicarrier systems," *Proc. IEEE SPAWC 2008*, pp. 525–529, Jul 2008.

[6] L. G. Baltar, D. S. Waldhauser, and J. A. Nossek, "MMSE subchannel decision feedback equalization for filter bank based multicarrier systems," *Proc. IEEE ISCAS 2009*, pp. 2802 – 2805, May 2009.

[7] D. S. Waldhauser, "Multicarrier systems based on filter banks," Ph.D. dissertation, Technische Universität München, Munich, Oct 2009.

[8] H. G. Göckler and A. Groth, *Multiratensysteme*. Schlembach Verlag, 2004.

[9] T. Karp and N. J. Fliege, "Computationally efficient realization of MDFT filter banks," *Proc. EUSIPCO '96*, vol. 2, pp. 1183–1186, Sep 1996.

[10] J. M. Cioffi, G. P. Dudevoir, M. Vedat Eyuboglu, and J. Forney, G. D., "MMSE decision-feedback equalizers and coding. I. Equalization results," *IEEE Trans. Commun.*, vol. 43, no. 10, pp. 2582 –2594, Oct 1995.

[11] M. G. Bellanger, "Specification and design of a prototype filter for filter bank based multicarrier transmission," in *Proc. IEEE ICASSP 2001*, Salt Lake City, USA, Mai 2001, pp. 2417–2420.